東北大学機関リポジトリ
TOUR
Tohoku University Repository
東北大学

Wavelength- and Tissue-dependent Variations in the Mutagenicity of Cyclobutane Pyrimidine Dimers in Mouse Skin

著者	Hironobu Ikehata, Toshio Mori, Yasuhiro Kamei, Thierry Douki, Jean Cadet, Masayuki Yamamoto
journal or publication title	Photochemistry and Photobiology
volume	96
page range	94-104
year	2019-08-28
URL	http://hdl.handle.net/10097/00128836

doi: 10.1111/php.13159

Wavelength- and Tissue-dependent Variations in the Mutagenicity of Cyclobutane Pyrimidine Dimers in Mouse Skin

Hironobu Ikehata*[1], Toshio Mori[2], Yasuhiro Kamei[3], Thierry Douki[4], Jean Cadet[5] and Masayuki Yamamoto[1]

[1] Department of Medical Biochemistry, Tohoku University Graduate School of Medicine, Sendai, Japan

[2] Nara Medical University School of Medicine, Kashihara, Japan

[3] Core Research Facilities, National Institute for Basic Biology, Okazaki, Japan

[4] Université Grenoble Alpes, CEA, CNRS, INAC, SyMMES/CIBEST, Grenoble, France

[5] University of Sherbrooke, Sherbrooke, Canada

*Corresponding author's e-mail: ikehata@med.tohoku.ac.jp (Hironobu Ikehata)

ABSTRACT

The cyclobutane pyrimidine dimer (CPD) is a main mutagenic photolesion in DNA produced by UVR. We previously studied the wavelength-dependent kinetics of mutation-induction efficiency using monochromatic UVR sources and transgenic mice developed for mutation assay and established the action spectra of UVR mutagenicity in the mouse epidermis and dermis. Here, we further established the action spectra of CPD and pyrimidine(6-4)pyrimidone photoproduct formation in the same tissues and in naked DNA using the same sources and mouse strain. Quantitative ELISA helped us estimate the photolesion formation efficiencies on a molecule-per-nucleotide basis. Using these action spectra, we confirmed that the UVR mutation mostly depends on CPD formation. Moreover, the mutagenicity of a CPD molecule (CPD mutagenicity) was found to vary by wavelength, peaking at approximately 313 nm in both the epidermis and dermis with similar wavelength-dependent patterns. Thus, the CPD formation efficiency is a main determinant of UVR mutagenicity in mouse skin, whereas a wavelength-dependent variation in the qualitative characteristics of CPD molecules also affects the mutagenic consequences of UVR insults. In addition, the CPD mutagenicity was always higher in the epidermis than in the dermis, suggesting different cellular responses to UVR between the two tissues irrespective of the wavelength.

INTRODUCTION

Ultraviolet radiation (UVR) is genotoxic and can cause mutations and cancers in exposed tissues, such as skin. The genotoxicity of UVR originates from its ability to form specific DNA base photolesions, and the major types of these photolesions are cyclobutane pyrimidine dimers (CPDs) and pyrimidine(6-4)pyrimidone photoproducts (64PPs) (1, 2). Among these photolesions, CPDs cause most of the mutations induced by UVR (3, 4) and are specified by C-to-T base substitutions at dipyrimidine sites, which are called the "UV signature" (5). The molecular mechanism of CPD-mediated mutations is believed to be the following: these mutations are induced via an error-free translesion DNA synthesis (TLS) over a deaminated cytosine-containing CPD, in which cytosine is converted to uracil, or via an error-prone TLS over a cytosine-containing CPD, which is mainly ruled by the A-rule (2, 6). However, the mutagenic efficiency of a CPD molecule (CPD mutagenicity) had been difficult to quantify precisely due to the lack of simultaneous quantitative analyses of mutagenicity and photolesion formation in a single system. Recently, we published one such analysis of CPD mutagenicity performed in mouse skin exposed to UVC and UVB using a quantitative ELISA for the determination of the molecular amounts of CPDs (7). In that study, we demonstrated that a CPD produced by UVB results in greater mutagenic consequences in the skin than a CPD produced by UVC.

UVR photolesions in DNA are produced through photochemical reactions between adjacent pyrimidine bases (1), and the reaction efficiency varies depending on the wavelength (8–14). However, whether the CPD mutagenicity also varies depending on the wavelength remains unclear. To answer this question, the absolute amounts of CPDs must be evaluated throughout the range of UVR wavelengths. The wavelength-dependent efficiency, namely, the action spectrum, of the formation of UVR photolesions was reported first as an integrated part of the so-called "average DNA spectrum" published by R. B. Setlow, which was a

combined action spectrum comprising phage/bacterial lethality and mutagenesis as well as photolesion formation in DNA (15). Since then, the action spectra of photolesion formation in UVR-irradiated DNA, phages, bacteria, mammalian cultured cells and human skin epidermis have been analyzed using chromatographic, immunological and photolesion-specific cleavage methods (8–14, 16–19). These action spectra are largely similar to the absorption spectrum of DNA, which demonstrates that CPDs and 64PPs are produced directly by the absorption of photon energy by DNA. However, most of these spectra are relatively obscure at long UVR wavelengths, such as those in the UVA region (320–400 nm) because they were evaluated using radiation sources with relatively poor resolution at these longer wavelengths (11, 16–19). More seriously, all of these spectra are less informative because their quantification of photolesions, which was mostly based on immunological assays, was not calibrated to absolute amounts of damage. For such a calibration, standard UVR-damaged DNA, whose absolute molecular amounts of photolesions are predetermined, is necessary. We recently developed a standard DNA whose photolesion amounts were quantified by HPLC with electrospray ionization tandem mass spectrometry (HPLC-ESI-MS/MS) and evaluated the absolute amounts of CPDs and 64PPs in mouse skin exposed to UVC and UVB through a quantitative ELISA assisted with the standard DNA (7). In the present study, we used this method to construct high-resolution action spectra of UVR photolesion formation in mouse skin that were calibrated to the absolute molecular amounts. With these spectra, we estimated the wavelength-dependent relationship of photolesion formation and UVR mutagenesis in the mouse skin by coupling with the action spectra of UVR mutagenicity in the skin that we previously established using transgenic mice developed for *in vivo* mutation analysis (20), and further analyzed the mutagenicity of CPD molecules.

MATERIALS AND METHODS

UVR sources. For the action spectrum studies, a high-power, high-resolution monochromatic UVR source, the Okazaki Large Spectrograph (OLS) (21), and a 364-nm UVA laser (22), both of which were available at the National Institute for Basic Biology (NIBB; Okazaki, Japan), were utilized. The detailed conditions for mouse irradiation with these sources have been described previously (20). Dosimetry was performed with a silicon photodiode (Hamamatsu Photonics, Hamamatsu, Japan).

Mice, DNA and UVR exposure. All procedures for the animal experiments, including husbandry, were approved by the Institutional Animal Care and Use Committees of Tohoku University and the National Institutes of Natural Sciences (NINS) (to which NIBB belongs) and conducted according to the Fundamental Guidelines for Proper Conduct of Animal Experiment and Related Activities in Academic Research Institutions under the jurisdiction of the Ministry of Education, Culture, Sports, Science and Technology of Japan and the Regulations for Animal Experiments and Related Activities at Tohoku University and NINS. Transgenic mice harboring λ-phage-based *lacZ* mutational reporter genes (23) were used for all the experiments. The dorsal skin of 8 to 12-week-old mice was depilated with an electric shaver and hair-removal cream (Kracie, Japan) and, three days later, the mice were exposed under anesthesia to monochromatic UVR at 260, 280, 290, 295, 300, 307, 313, 319, 325, 330 and 334 nm emitted from the OLS. The spectral half-power bandwidths were ± 2.7 nm at all wavelengths. At wavelengths ≥ 307 nm, appropriate cutoff filters were used to remove stray shorter-wavelength radiations. For the analysis at 364 nm, we utilized the DNA samples obtained from mouse skin exposed to a 364-nm laser in one of our previous studies (22). Calf thymus DNA (Sigma-Aldrich) dissolved to a concentration of 1 mg/ml in a solution consisting of 10 mM Tris-HCl (pH 8.0) and 1 mM EDTA was also irradiated at each wavelength of the monochromatic UVR from the OLS in a plastic dish covered with an

ND90 quartz filter, which prevented the solution from evaporating out. The OLS conditions and filters used for DNA irradiation were the same as those used for mice. Exposure of the DNA solution to the 364-nm laser was not performed because the laser apparatus had been broken and was no longer available.

DNA damage assay. The mice were sacrificed immediately after UVR exposure to excise the irradiated skin area. After the DNA metabolic activities in the excised skin section were inactivated by incubation at 55°C for 5 min, the epidermis of the skin section was separated from the dermis with thermolysin, and the epidermal and dermal genomic DNA was isolated from each tissue (24). The absolute amounts of CPDs and 64PPs in the DNA were determined quantitatively based on the number of molecules per nucleotide using a recently developed ELISA-based method calibrated with the standard UVR-exposed DNA (7) whose photolesion amounts were predetermined by HPLC-ESI-MS/MS (24). The ELISA was performed with monoclonal antibodies specific to CPDs and 64PPs, TDM-2 and 64M-2, respectively, and the color development reactions were assayed at 450 nm using a Sunrise microplate reader (Tecan, Austria), as described previously (7).

Action spectra of UVR mutagenicity in mouse skin. We previously analyzed the action spectra of mutation induction (mutagenicity) in mouse skin by determining dose-response kinetics of increases in mutant frequencies (MFs) in the epidermis and dermis after exposure to UVR; in these analyses, the MFs of the *lacZ* transgene were evaluated using the transgenic mice mentioned above (20). In the present study, these data were utilized for quantitative evaluation of the efficiency with which photolesions induce mutations in the skin.

RESULTS

Dose-response kinetics of photolesion formation in mouse skin

The depilated dorsal skin of groups of mice was exposed to a series of doses of monochromatic UVR at select wavelengths from 260 to 364 nm, and the mice were sacrificed immediately to estimate the amounts of photoinduced CPDs and 64PPs in the epidermis and dermis of their exposed skin sections. Solutions of naked DNA were also exposed to several doses of monochromatic UVR at the same wavelengths except 364 nm. The photolesion amounts were evaluated on a molecule-per-nucleotide basis through a quantitative ELISA calibrated with standard UVR-damaged DNA, and the results were plotted to reveal the dose-response kinetics (Fig. 1). Regression lines for these dose-response kinetics were estimated to deduce the amounts of each photolesion formed by a unit dose of UVR at each wavelength, namely, slopes of the induction of photolesion formation, under the premise that the *y*-intercept is null ([photolesion amount] = a*[UVR dose]). Some data points at higher doses were excluded from the estimation because they deviated largely from the estimated regression line and showed lower amounts than expected. Those excluded points for 64PP were outside of the lesion amount range that was reliably quantifiable using the standard DNA for calibration ($\leq$ 50 molecules per 10^6 bases) (7), whereas the points for CPD were expected to show more than 300 lesions per 10^6 bases with the regression analysis, which appears to be a limit for the reliable estimation of CPD amounts using the quantification method as reported previously (7). The slopes estimated for 64PP at wavelengths greater than 325 nm were not used for further analysis because significant increases in 64PP were not observed at these wavelengths (Fig.1b, c). Regression analyses confirmed the significance of all the regressions (ANOVA, $p < 0.001$ for all except the followings: epidermal CPD at 260 nm, $p = 0.00102$; epidermal and dermal 64PP at 325 nm, $p = 0.031$ and 0.0033, respectively; and dermal CPD at 334 nm, $p = 0.0024$) except those for 64PP at wavelengths greater than 325 nm.

Action spectra of UVR photolesion formation in mouse skin

Based on the slopes obtained from the regression analyses shown in Fig. 1, action spectra of the efficiency of UVR photolesion formation in naked DNA and in mouse epidermis and dermis were estimated (Fig. 2a and Fig. S1a, see Supporting Materials). The efficiencies of photolesion formation were highest and paralleled one another at wavelengths from 260 to 290 nm in DNA and the epidermis whereas a peak appeared at 295 nm in the dermis. The decreased efficiencies at the shorter wavelengths in the dermis would have resulted from less efficient transmission of the shorter-wavelength UVR through the epidermal layer (19, 26).

The action spectra of CPD formation were nearly identical among the epidermis, dermis and DNA at wavelengths longer than 295 nm, whereas those of 64PP formation differed between DNA and the two skin tissues in the same wavelength region (Fig. 2b). Although most of these action spectra diverged at wavelengths shorter than 295 nm (Fig. 2b), the differences between the epidermis and dermis would reflect UVR protection by the epidermal layer at these wavelengths (19, 26). The almost identical action spectra of CPD and 64PP formation obtained for the two skin tissues in the longer wavelength range indicate the efficient transmittance of 300-nm or longer UVR photons through the epidermal layer of mouse skin, which was previously reported for human skin (19, 27, 28), confirming the poor protection by the epidermis against the long-wavelength UVR included in the UVB and UVA ranges. The different action spectra of 64PP formation between DNA and the skin tissues indicate that 64PP formation is less efficient in naked DNA than in cellular DNA in the skin tissues at wavelengths between 300 and 320 nm (Fig. 2b, 64PP). Although the efficiencies of 64PP formation were comparable between DNA and the epidermis at wavelengths shorter than 295 nm, this observation might be a coincidence because the epidermal cornified layer should attenuate UVR at these shorter wavelengths (19, 26–28). This attenuation effect is clearly evidenced by the action spectra of CPD formation (Fig. 2b, CPD), which showed less

efficient CPD formation in the epidermis than in DNA, revealing the protection ability of the cornified layer against short-wavelength UVR. Thus, the protection against 64PP formation by the epidermal cornified layer would have negated the more efficient 64PP formation in the epidermis, resulting in the similar efficiencies in 64PP formation.

The efficiencies of CPD formation were always higher than the efficiencies of 64PP formation throughout the wavelengths examined, and the differences appeared to become greater as the wavelength increased until 64PP formation decreased to barely detectable levels at 325 nm (Fig. 2a). The difference in the efficiencies of CPD and 64PP formation in the skin tissues was relatively constant between 260 and 300 nm, as shown by the molecular ratios of 64PPs to CPDs in Fig. 2c (*ca.* 0.2 and 0.1 for the epidermis and dermis, respectively). The smaller ratios in the dermis than in the epidermis may reflect less efficient 64PP formation in the former, which might have resulted from some difference in the cellular DNA structures between the two tissues that could affect 64PP formation. From 300 nm, the difference in the efficiencies of CPD and 64PP formation accelerated as the wavelength increased (Fig. 2c), suggesting a mechanistic difference in photolesion formations between the shorter and longer wavelength ranges. The profile of photolesion formation in naked DNA was slightly different from those in the skin: the difference in the efficiencies of CPD and 64PP formation started increasing from a shorter wavelength of 290 nm, but the acceleration of the difference was weaker than those of the skin (Fig. 2c).

Comparison of action spectra of photolesion formation and mutagenesis

The action spectra of CPD and 64PP formation in mouse skin were compared with the action spectra of mutation induction (mutagenicity) by UVR that we had previously analyzed with the same UVR sources used in the present study (20) (Fig. 3, see also Fig. S1b). The action spectra of the mutagenicity closely paralleled the CPD formation spectra in both the

epidermis and dermis at 295 nm and longer wavelengths, but did not parallel the 64PP formation spectra at wavelengths longer than 300 nm, which indicates that CPD is most likely the photolesion contributing to UVR mutagenesis, confirming previous studies (3, 4). On the other hand, the mutagenicity of 64PP was not supported by the action spectrum analysis shown here. The disagreements between damage and mutagenicity spectra at wavelengths shorter than 295 nm may reflect the gradational production of CPDs along the skin depth in this short-wavelength range (27), which is discussed in the Discussion section.

Molecular mutagenicity of CPDs in mouse skin

To estimate the wavelength dependence of the mutagenicity of a CPD molecule (CPD mutagenicity) in the mouse epidermis and dermis, wavelength-dependent increases in the MF of the *lacZ* transgene per unit dose of UVR, which had been evaluated in each tissue in our previous study (20), were divided by the number of CPD molecules produced in a *lacZ* gene (assumed to be 6000 bases), which were deduced from the data obtained with the quantitative ELISA (Fig. 1a, b). The calculation was performed at every wavelength examined, and the results were plotted (Fig. 4a). The CPD mutagenicity changed in a wavelength-dependent manner with similar patterns in the epidermis and dermis, which exhibited an increase between 295 and 330 nm with a peak at approximately 313 nm. Interestingly, CPD mutagenicity was always higher in the epidermis than in the dermis. The ratios of CPD mutagenicity in the epidermis to that in the dermis are relatively constant (2.55 ± 0.81) at all the wavelengths examined except 260 nm (Fig. 4b). The large error in the CPD mutagenicity ratio at 260 nm resulted from the small amount of CPDs in the dermis that was close to the detection limit of the ELISA.

Amount of photolesions for the induction of MIS responses

Although UVR induces mutations and increases MF in the skin genome, UVR doses larger than a certain amount trigger a remarkable response in the epidermis that the MF increase stops and levels off to a constant MF (20, 29). This response is called "mutation induction suppression" (MIS), which is thought to be an epidermis-specific response related to apoptosis and hyperplasia (30). Because the minimum doses for induction of the MIS response at the wavelengths examined here were previously evaluated (20), the minimum amounts of CPDs and 64PPs necessary to induce the MIS response were estimated using data obtained in the present study and plotted to examine their wavelength dependency (Fig. 5). The estimated amounts of photolesions required to induce MIS exhibited variations among wavelengths, especially did the amount of CPDs, increasing remarkably in the range of 295–334 nm. The increases in 64PPs appeared to be relatively small, but their fold changes were comparable to those for CPD. Thus, the photolesion amounts showed notable differences among wavelengths when the MIS response starts. It does not appear that the amount of CPDs or 64PPs alone is the determinant to trigger the MIS response.

DISCUSSION

Action spectra of UVR photolesion formation

Previous studies on the action spectra of the formation of UVR photolesions were performed mainly for CPDs using *in vitro* systems such as DNA solutions (9, 11, 13, 14) and suspensions of bacteria (10) and mammalian cultured cells (8, 12, 16, 18), although some of these studies were also focused on 64PPs (11–14). Similar studies have also been performed *in vivo* using human skin (17, 19), but these analyses were performed for CPD formation alone using UVR sources with a relatively poor wavelength resolution in the UVA region. In the present study, we established the action spectra of photolesion formation in the skin *in*

256 *vivo* for both CPDs and 64PPs with a high wavelength resolution into the UVA range and
257 comparable action spectra of photolesion formation in DNA *in vitro*.

258 The efficiency of photolesion formation in the epidermis was constant for both CPDs
259 and 64PPs at wavelengths from 260 to 290 nm. The same trend was also observed for the
260 action spectra of DNA (Fig. 2a, DNA and Epidermis), which was surprising because the
261 absorption spectrum of DNA peaks at approximately 260 nm. Because photolesion formation
262 is initiated by photon absorption by relevant molecules, its action spectrum would be
263 expected to peak at the same wavelength as the absorption spectrum. Although this
264 unexpected observation might result from some artificially imposed experimental conditions,
265 such as the concentration of DNA exposed to UVR, which might have been relatively too
266 high (1 mg/ml) in the present study for homogeneous photon absorption in the DNA solution
267 at these short wavelengths, some photochemical and biochemical interactions may be
268 involved. Similar trends of the flat efficiencies in the short-wavelength region were
269 detectable in some previous action spectrum studies (8, 9, 11, 13) and were actually observed
270 in a previous photochemical study (31). The flat spectra suggest that the yield of photolesions
271 is not proportional to the absorption coefficients of DNA in this short wavelength range.
272 Photoreversal reactions of photolesions, which have been actually observed for CPDs (32,
273 33), could partly contribute to the observation.

274 On the other hand, we observed a peak at 295 nm in the action spectra of both CPD and
275 64PP formation in the dermis (Fig. 2a, Dermis). The peak can be explained by the epidermal
276 layer preventing the penetration of UVR at wavelengths shorter than 295 nm into the dermis.
277 Similar observations have been reported for human skin (17, 19); the action spectra for CPD
278 formation in the epidermis showed peaks at approximately 300 nm. In human skin, the upper
279 differentiated cell layers are thought to function as UVR barriers because the human

epidermis is multicell-layered and much thicker than the mouse epidermis, which usually consists of one or two cell layers.

Difference in 64PP formation spectra between DNA and skin

We noticed a difference in the action spectra of 64PP formation between naked DNA and mouse skin tissues in contrast to the almost identical action spectra of CPD formation between them except at shorter wavelengths (Fig. 2b). At wavelengths between 300 and 313 nm, for which protection by skin layers is almost negligible (19, 27, 28), the efficiencies of 64PP formation in the skin were several-fold higher than those in naked DNA, which indicates that 64PP forms more easily in skin DNA, *i.e.*, in cellular DNA, than in naked DNA dissolved in water when the midrange UVR is used. Because the similarly or less efficient 64PP formation at the short wavelengths in the skin would have resulted from the previously mentioned UVR attenuation by the upper layers of skin, the higher 64PP formation efficiency in cellular DNA than in naked DNA could be expanded to the short UVR range. Higher efficiencies of photolesion formation in cellular DNA than in naked DNA were also observed in a previous study (34). Although the cause of the different 64PP formation efficiencies between cellular and naked DNA is currently unknown, some differences in their DNA structures might have affected the 64PP formation efficiency. It is known that the distribution of 64PP formation in cellular DNA, which takes a chromatin structure with histone proteins, is not uniform and differs from that in naked DNA (35), and that differences in base stacking, which shows variability depending on the DNA duplex conformation, significantly affect the efficiency of UVR photolesion formation, particularly the formation of 64PPs (36, 37).

At 313 nm, the situation was reversed. At longer wavelengths, in contrast to the sharp decreases in 64PP formation efficiency in skin tissues, the decrease in the efficiency in naked DNA became gradual, which resulted in a higher efficiency in naked DNA at 325 nm (Fig. 2b,

64PP). Similar wavelength-dependent 64PP formation in naked DNA was observed previously (13). Because UVR at these wavelengths converts 64PPs to Dewar valence isomers (13, 38, 39), the gradual decrease in the 64PP formation efficiency may indicate less efficient isomerization in naked DNA than in cellular DNA. Actually, the rigidness and/or strandedness of the backbone structure of DNA, which could vary by chromosomal conformation, affects the yield of Dewar isomers from 64PPs (40, 41). The accelerated decreases in 64PP formation efficiency in the skin tissues compared with naked DNA (Fig. 2b, c) confirm the efficient conversion of 64PPs to Dewar isomers in cellular DNA suggested in previous studies at these longer wavelengths (12, 38, 42).

Difference in action spectra between CPD and 64PP formations

The action spectra of CPD and 64PP formation were quite similar at wavelengths up to 290 nm (DNA) or 300 nm (skin) but increasingly diverged as the wavelength increased further (Fig. 2a, Fig. 3), although the diversion in naked DNA was smaller than that in the skin. 64PP formation was hardly detectable at wavelengths longer than 325 nm, probably due to an energy barrier for 64PP production (31) and efficient conversion to Dewar isomers by UVR (12, 13, 38) at these longer wavelengths. In contrast, the decrease in the efficiency of CPD formation was alleviated in the UVA1 range (340–400 nm) and still detectable at wavelengths up to 364 nm. At wavelengths shorter than 300 nm, CPDs and 64PPs are produced mainly through a similar initial photochemical excitation of pyrimidine bases to a singlet state (31), which would have resulted in similar action spectra of formation for these photolesions although their formation efficiencies are different with a relatively constant ratio in each tissue or naked DNA (Fig. 2c). However, the following photochemical reactions for the production of CPDs and 64PPs are different because $\pi\pi^*$ and charge-transfer excited states are involved, respectively (31). The latter process has a large energy barrier for the

production of 64PPs, which could decrease the production efficiency at wavelengths longer than 290 nm, as observed for the thymidine polynucleotide $(dT)_{20}$ (31). The tailing of CPD formation spectra in the UVA range would reflect a photochemical reaction process different from the singlet ππ* excitation, which is another charge-transfer excited state called "collective excitation" that occurs in double-stranded DNA at a very low efficiency but with low photon energies, in contrast to ππ* excitation (43, 44), and is thus detectable only at low-energy wavelengths such as those in UVA1. Little or no detection of 64PPs/Dewar isomers and low but significant production of CPDs in the UVA region have actually been observed for DNA, cells and skin tissues in studies with polychromatic UVR sources (45–48).

We observed relatively constant molecular ratios between CPDs and 64PPs at wavelengths up to 290 (naked DNA) or 300 nm (skin DNA): 5- to 10-fold more CPDs compared with 64PPs (Fig. 2c). This difference is a greater than those reported in one of our previous studies performed with HPLC-ESI-MS/MS (*ca*. 3-fold more CPDs) for naked and cellular DNA using conventional UVC and UVB sources (34). In another study, however, we observed a 64PP/CPD ratio of 0.07 in UVB-irradiated naked DNA, which was used as the standard UVR-damaged DNA for our quantitative ELISA, with the same mass spectrometry-based method and reported the formation of 5- to 10-fold or more CPDs than 64PPs in UVB- or UVC-exposed mouse skin with the ELISA (7). Similar 64PP/CPD ratios have also been observed for the quantum yields of both photolesions in a photochemical study with $(dT)_{20}$ (31). In addition, we noticed consistently lower 64PP/CPD ratios in the dermis than in the epidermis irrespective of the UVR source in the UVC and UVB ranges (Fig. 2c) (7), which suggests less efficient 64PP formation in the dermis than in the epidermis because the CPD formation efficiencies are comparable between these tissues (Fig. 2b). The conformation of nuclear DNA in dermal fibroblasts might be less susceptible to 64PP formation than that in epidermal keratinocytes.

Similarities and differences in action spectra between photolesion formation and mutagenicity

The damage formation action spectra paralleled the mutagenicity spectra for CPD but not that for 64PP in both the epidermis and dermis at wavelengths of 295 nm or longer (Fig. 3). At shorter wavelengths, however, substantial differences appeared between the spectra: mutation inducibility was less efficient than photolesion formation. This difference could result from the ability of the cornified/epidermal layers to prevent the transmission of these short wavelengths (19, 26–28), which would cause a gradient in photolesion distribution with less photolesion content at deeper regions of skin tissues, as observed previously (27). In this situation, heavily damaged cells would be eliminated by apoptosis or some other cell-killing mechanisms, whereas less-damaged cells would survive to reconstitute the damaged skin tissue. In our analysis, the mutations in UVR-exposed skin areas were assayed 4 weeks after irradiation, and thus, only the less-damaged surviving cells would have contributed to the mutagenicity spectra, resulting in mutagenic efficiencies that were lower than photolesion formation efficiencies in the short wavelength range. On the other hand, because skin layers are transparent to UVR at wavelengths longer than 300 nm (19, 27, 28), the distribution of photolesions would be largely homogeneous among cells throughout each skin tissue, resulting in similar action spectra between CPD formation and mutagenicity at these longer wavelengths (Fig. 3).

The action spectra of 64PP formation were quite different from the mutagenicity spectra not only at the shorter wavelengths but also in the longer-wavelength UVR region (Fig. 3), which suggests a poor contribution of 64PPs to UVR-induced mutagenesis, at least in the skin of wild-type mice that were used in the present study. Although several studies reported some contributions of 64PP to UVR mutagenicity (49–51), these mutagenicities

were detected in some particular situations, such as in a mutagenic adaptive response (49, 51) and/or DNA repair deficiency (49–51). 64PPs are removed rapidly from the UVR-damaged mammalian genome by DNA repair (52, 53), whereas CPDs are slowly or hardly removed from mammalian cells and the skin (52–55). In fact, under repair-proficient, ordinary conditions, CPDs are major photolesions that induce UVR-specific mutations (3, 4). These studies indicate that the mutagenicity of 64PP should depend on the repair proficiency and emerge under defective photolesion removal. Because we used repair-proficient mice in the present study, it is not surprising that the action spectra supported CPD dominance in UVR mutagenicity.

Wavelength dependence of CPD mutagenicity

Because we assessed that CPDs but not 64PPs mainly contribute to mutagenicity in normal skin, the molecular mutagenicity of CPD in mouse skin has been estimated based on the action spectra of CPD formation and that of mutagenicity established in our previous studies (20) and found to exhibit a similar wavelength-dependent variation in both the epidermis and dermis, with a peak at approximately 313 nm (Fig. 4a). The mutagenicity of CPD depends on combinations of dimerized pyrimidines: cytosine-containing CPDs are mutagenic and produce UV-signature mutations (2, 5), whereas cyclobutane thymine dimers rarely induce mutations in cultured cells and skin (2). Moreover, among cytosine-containing CPDs, those formed in the 5'-TCG-3' sequence are known to be most mutagenic (56) due to their exceptionally high tendency for cytosine deamination in the CPD (57, 58). Cytosine deamination in CPDs produces uracil-containing CPDs that can induce C-to-T mutations via TLS. In addition, the distribution of mutation recoveries among dipyrimidine-containing triplet sequences shows a wavelength-dependent variation especially at the 5'-TCG-3' sequence, which shifts the mutation spectrum between the "UV signature" and "UVA

405 signature" (56). The 5'-TCG-3' sequence includes a CpG motif, which is the target sequence
406 of DNA methylation, an epigenetic DNA modification specific to vertebrate genomes (59). It
407 is known that the frequency of CPD formation at the CpG motif varies depending on its
408 methylation status and the wavelength of incident UVR (60–63): UVB and/or sunlight UVR
409 preferably produce CPDs at dipyrimidine-associated, methylated CpG sites in contrast to
410 UVC (60, 61, 63). Thus, mutagenic subclasses of CPDs, mostly cytosine-containing, CpG-
411 associated CPDs, are produced in a wavelength-dependent manner, which leads to the
412 wavelength-dependent variation in the mutation signature (56) and CPD mutagenicity
413 observed in this study. We previously reported that exposure to UVB produced CPDs with a
414 higher molecular mutagenicity in mouse skin than exposure to UVC (7). The present study
415 confirmed this result and characterized the profile of CPD mutagenicity more precisely as a
416 unique wavelength-dependent pattern that peaks at approximately 313 nm (Fig. 4a). Because
417 the wavelength-dependent patterns are quite similar between the epidermis and dermis, the
418 mechanisms of CPD-mediated mutagenesis should be common in both tissues.
419 In summary, the present study confirmed that CPD is a major mutation-causing
420 photolesion throughout the UVR region from 260 to 364 nm. The efficiency of CPD
421 formation is proportionally correlated with the efficiency of mutation induction as directly
422 evidenced in Fig. 3. Thus, UVR mutagenicity appears to be determined mainly by the CPD
423 formation efficiency. However, the wavelength-dependent variation in the mutagenicity of a
424 CPD molecule shown in Fig. 4a reveals that the quality of CPD, such as its base composition
425 and locating sequence context, can also influence UVR mutagenicity, although this
426 contribution is relatively minor. Thus, both the formation efficiency and the molecular quality
427 of CPD affect the wavelength dependence of the UVR-induced mutation.
428
429 **Different CPD mutagenicities between the epidermis and dermis**

Although the wavelength dependence in the epidermis and dermis shows parallel patterns, CPD mutagenicities are always higher in the epidermis than in the dermis (Fig. 4a) and constantly 2- to 3-fold higher at wavelengths longer than 260 nm (Fig. 4b). Similar differences were observed in our previous study with conventional UVC and UVB lamps (7). The lower mutagenicity in the dermis might suggest more efficient DNA repair, which is, however, inconsistent with previous studies (64–66), which supported a superiority of the epidermis in CPD removal. The UVR-damaged epidermis shows rapid tissue turnover, such as the MIS response, inducing extensive apoptosis followed by hyperplasia with active proliferation of less-damaged, surviving keratinocytes (30, 67), which would result in mutation fixation mediated through the TLS of CPDs remaining in the surviving cells. Although the cellular kinetics in the dermis after UVR insults have not been clarified, the following interesting observation was reported: partial or local elimination of dermal fibroblasts by laser or toxin does not induce cell proliferation or repopulation from surrounding areas but rather encourages the remaining fibroblasts to extend their cell membrane into the depleted regions without changing their location to maintain the cellular networks in the dermis (68). If the same response does occur after UVR insult, such active cell proliferation in the epidermis would not be expected in the dermis, which would result in fewer mutations in the dermis than in the epidermis, as observed in the present study.

We previously reported that the epidermis exhibits the MIS response after an exposure to high doses of UVR. In this response, the dose-dependent increase in the MF stops and plateaus at a constant level (plateau MF) above a certain UVR dose (20, 29). The plateau MF varies depending on the wavelength of the UVR, peaking at 313 nm with a similar pattern as the wavelength dependence of CPD mutagenicity observed in this study (20). However, the wavelength-dependent variation in the plateau MF cannot be explained by that of CPD mutagenicity alone because their degrees of variation are fairly different (roughly 20-fold *vs.*

5-fold, respectively). Although the remaining variation in the plateau MF can be explained by the different number of CPDs produced at each wavelength when the MIS response is induced (Fig. 5), the CPD numbers do not appear to determine the timing of the response. Other wavelength-dependent UVR sensors that induce extensive apoptosis in the epidermis should trigger the MIS response.

Acknowledgements—We thank T. Uchikawa, S. Higashi, Y. Hasegawa and Y. Takahashi for the experimental assistance provided. This work was performed under the NIBB Cooperative Research Program for the Okazaki Large Spectrograph (11-501, 12-501, 13-501, 14-501, 15-601, 16-701 and 17-701) and was supported by JSPS KAKENHI Grant Numbers 15H02815 to H. Ikehata and 19H05649 to M. Yamamoto.

SUPPORTING MATERIALS

Figure S1 can be found at DOI: xxxx-xxxxxx.s1.

REFERENCES

1. Cadet, J., E. Sage and T. Douki (2005) Ultraviolet radiation-mediated damage to cellular DNA. *Mutat. Res.* **571**, 3–17.
2. Ikehata, H. and T. Ono (2011) The mechanisms of UV mutagenesis. *J. Radiat. Res.* **52**, 115–125.
3. You, Y., D. Lee, J. Yoon, S. Nakajima, A. Yasui and G. P. Pfeifer (2001) Cyclobutane pyrimidine dimers are responsible for the vast majority of mutations induced by UVB irradiation in mammalian cells. *J. Biol. Chem.* **276**, 44688–44694.
4. Jans, J., W. Schul, Y.-G. Sert, Y. Rijksen, H. Rebel, A. P. M. Eker, S. Nakajima, H. van Steeg, F. R. de Gruijl, A. Yasui, J. H. J. Hoeijmakers and G. T. J. van der Horst (2005) Powerful skin cancer protection by a CPD-photolyase transgene. *Curr. Biol.* **15**, 105–115.
5. Brash, D. E., J. A. Rudolph, J. A. Simon, A. Lin, G. J. McKenna, H. P. Baden, A. J. Halperin and J. Pontén (1991) A role for sunlight in skin cancer: UV-induced p53 mutations in squamous cell carcinoma. *Proc. Natl Acad. Sci. USA* **88**, 10124–10128.
6. You, Y. and G. P. Pfeifer (2001) Similarities in sunlight-induced mutational spectra of CpG-methylated transgenes and the *p53* gene in skin cancer point to an important role of 5-methylcytosine residues in solar UV mutagenesis. *J. Mol. Biol.* **305**, 389–399.
7. Ikehata, H., T. Mori, T. Douki, J. Cadet and M. Yamamoto (2018) Quantitative analysis of UV photolesions suggests that cyclobutane pyrimidine dimers produced in mouse skin by UVB are more mutagenic than those produced by UVC. *Photochem. Photobiol. Sci.* **17**, 404–413.
8. Rothman, R. H. and R. B. Setlow (1979) An action spectrum for cell killing and pyrimidine dimer formation in Chinese hamster V-79 cells. *Photochem. Photobiol.* **29**, 57–61.

9. Ellison, M. J. and J. D. Childs (1981) Pyrimidine dimers induced in *Escherichia coli* DNA by ultraviolet radiation present in sunlight. *Photochem. Photobiol.* **34**, 465–469.
10. Peak, M. J., J. G. Peak, M. P. Moehring and R. B. Webb (1984) Ultraviolet action spectra for DNA dimer induction, lethality, and mutagenesis in *Escherichia coli* with emphasis on the UVB region. *Photochem. Photobiol.* **40**, 613–620.
11. Chan, G. L., M. J. Peak, J. G. Peak and W. A. Haseltine (1986) Action spectrum for the formation of endonuclease-sensitive sites and (6-4) photoproducts induced in a DNA fragment by ultraviolet radiation. *Int. J. Radiat. Biol.* **50**, 641–648.
12. Rosenstein, B. S. and D. L. Mitchell (1987) Action spectra for the induction of pyrimidine(6-4)pyrimidone photoproducts and cyclobutane pyrimidine dimers in normal human skin fibroblasts. *Photochem. Photobiol.* **45**, 775–780.
13. Matsunaga, T., K. Hieda and O. Nikaido (1991) Wavelength dependent formation of thymine dimers and (6-4)photoproducts in DNA by monochromatic ultraviolet light ranging from 150 to 365 nm. *Photochem. Photobiol.* **54**, 403–410.
14. Besaratinia, A., J. Yoon, C. Schroeder, S. E. Bradforth, M. Cockburn and G. P. Pfeifer (2011) Wavelength dependence of ultraviolet radiation-induced DNA damage as determined by laser irradiation suggests that cyclobutane pyrimidine dimers are the principal DNA lesions produced by terrestrial sunlight. *FASEB J.* **25**, 3079–3091.
15. Setlow, R. B. (1974) The wavelengths in sunlight effective in producing skin cancer: a theoretical analysis. *Proc. Natl Acad. Sci. USA* **71**, 3363–3366.
16. Enninga, I., R. T. L. Groenendijk, A. R. Filon, A. A. van Zeeland and J. W. I. M. Simons (1986) The wavelength dependence of u.v.-induced pyrimidine dimer formation, cell killing and mutation induction in human diploid skin fibroblasts. *Carcinogenesis* **7**, 1829–1836.

17. Freeman, S. E., H. Hacham, R. W. Gange, D. J. Maytum, J. C. Sutherland and B. M. Sutherland (1989) Wavelength dependence of pyrimidine dimer formation in DNA of human skin irradiated *in situ* with ultraviolet light. *Proc. Natl Acad. Sci. USA* **86**, 5605–5609.
18. Kielbassa, C., L. Roza and B. Epe (1997) Wavelength dependence of oxidative DNA damage induced by UV and visible light. *Carcinogenesis*, **18**, 811–816.
19. Young, A. R., C. A. Chadwick, G. I. Harrison, O. Nikaido, J. Ramsden and C. S. Potten (1998) The similarity of action spectra for thymine dimers in human epidermis and erythema suggests that DNA is the chromophore for erythema. *J. Invest. Dermatol.* **111**, 982–988.
20. Ikehata, H., S. Higashi, S. Nakamura, Y. Daigaku, Y. Furusawa, Y. Kamei, M. Watanabe, K. Yamamoto, K. Hieda, N. Munakata and T. Ono (2013) Action spectrum analysis of UVR genotoxicity for skin: the border wavelengths between UVA and UVB can bring serious mutation loads to skin. *J. Invest. Dermatol.* **133**, 1850–1856.
21. Watanabe, M., M. Furuya, Y. Miyoshi, Y. Inoue, I. Iwahashi and K. Matsumoto (1982) Design and performance of the Okazaki Large Spectrograph for photobiological research. *Photochem. Photobiol.* **36**, 491–498.
22. Ikehata, H., K. Kawai, J. Komura, K. Sakatsume, L. Wang, M. Imai, S. Higashi, O. Nikaido, K. Yamamoto, K. Hieda, M. Watanabe, H. Kasai and T. Ono (2008) UVA1 genotoxicity is mediated not by oxidative damage but by cyclobutane pyrimidine dimers in normal mouse skin. *J. Invest. Dermatol.* **128**, 2289–2296.
23. Gossen, J. A., W. J. F. de Leeuw, C. H. T. Tan, E. C. Zwarthoff, F. Berends, P. H. M. Lohman, D. L. Knook and J. Vijg (1989) Efficient rescue of integrated shuttle vectors from transgenic mice: a model for studying mutations *in vivo*. *Proc. Natl Acad. Sci. USA* **86**, 7971–7975.

24. Ikehata, H., Y. Saito, F. Yanase, T. Mori, O. Nikaido and T. Ono (2007) Frequent recovery of triplet mutations in UVB-exposed skin epidermis of *Xpc*-knockout mice. *DNA Repair* **6**, 82–93.
25. Douki, T., M. Court, S. Sauvaigo, F. Odin and J. Cadet (2000) Formation of the main UV-induced thymine dimeric lesions within isolated and cellular DNA as measured by high performance liquid chromatography-tandem mass spectrometry. *J. Biol. Chem.* **275**, 11678–11685.
26. Bruls, W. A. G., H. Slaper, J. C. van der Leun and L. Berrens (1984) Transmission of human epidermis and stratum corneum as a function of thickness in the ultraviolet and visible wavelengths. *Photochem. Photobiol.* **40**, 485–494.
27. Chadwick, C. A., C. S. Potten, O. Nikaido, T. Matsunaga, C. Proby and A. R. Young (1995) The detection of cyclobutane thymine dimers, (6-4) photolesions and Dewar photoisomers in sections of UV-irradiated human skin using specific antibodies, and the demonstration of depth penetration effects. *J. Photochem. Photobiol. B: Biol.* **28**, 163–170.
28. Therrien, J.-P., M. Rouabhia, E. A. Drobetsky and R. Drouin (1999) The multilayered organization of engineered human skin does not influence the formation of sunlight-induced cyclobutane pyrimidine dimers in cellular DNA. *Cancer Res.* **59**, 285–289.
29. Ikehata, H. and T. Ono (2002) Mutation induction with UVB in mouse skin epidermis is suppressed in acute high-dose exposure. *Mutat. Res.* **508**, 41–47.
30. Ikehata, H., R. Okuyama, E. Ogawa, S. Nakamura, A. Usami, T. Mori, K. Tanaka, S. Aiba and T. Ono (2010) Influences of p53 deficiency on the apoptotic response, DNA damage removal and mutagenesis in UVB-exposed mouse skin. *Mutagenesis* **25**, 397–405.

31. Banyasz, A., T. Douki, R. Improta, T. Gustavsson, D. Onidas, I. Vayá, M. Perron and D. Markovitsi (2012) Electronic excited states responsible for dimer formation upon UV absorption directly by thymine strands: joint experimental and theoretical study. *J. Am. Chem. Soc.* **134**, 14834–14845.
32. Deering, R. A. and R. B. Setlow (1963) Effects of ultraviolet light on thymidine dinucleotide and polynucleotide. *Biochim. Biophys. Acta*, **68**, 526–534.
33. Garcès F. and C. A. Davila (1982) Alterations in DNA irradiated with ultraviolet radiation I. The formation process of cyclobutylpyrimidine dimers: cross sections, action spectra and quantum yields. *Photochem. Photobiol.*, **35**, 9–16.
34. Douki, T. and J. Cadet (2001) Individual determination of the yield of the main UV-induced dimeric pyrimidine photoproducts in DNA suggests a high mutagenicity of CC photolesions. *Biochemistry* **40**, 2495–2501.
35. Mao, P., J. J. Wyrick, S. A. Roberts and M. J. Smerdon (2017) UV-induced DNA damage and mutagenesis in chromatin. *Photochem. Photobiol.* **93**, 216–228.
36. Improta, R. (2012) Photophysics and photochemistry of thymine deoxy-dinucleotide in water: a PCM/TD-DFT quantum mechanical study. *J. Phys. Chem. B* **116**, 14261–14274.
37. Martinez-Fernández, L. and R. Improta (2018) Sequence dependence on DNA photochemistry: a computational study of photodimerization pathways in TpdC and dCpT dinucleotides. *Photochem. Photobiol. Sci.* **17**, 586–591.
38. Mitchell, D. L. and B. S. Rosenstein (1987) The use of specific radioimmunoassays to determine action spectra for the photolysis of (6-4) photoproducts. *Photochem. Photobiol.* **45**, 781–786.
39. Douki, T. and E. Sage (2016) Dewar valence isomers, the third type of environmentally relevant DNA photoproducts induced by solar radiation. *Photochem. Photobiol. Sci.* **15**, 24–30.

40. Haiser, K., B. P. Fingerhut, K. Heil, A. Glas, T. T. Herzog, B. M. Pilles, W. J. Schreier, W. Zinth, R. de Vivie-Riedle and T. Carell (2012) Mechanism of UV-induced formation of Dewar lesions in DNA. *Angew. Chem. Int. Ed.* **51**, 408–411.
41. Bucher, D. B., B. M. Pilles, T. Carell and W. Zinth (2015) Dewar lesion formation in single- and double-stranded DNA is quenched by neighboring bases. *J. Phys. Chem. B* **119**, 86865–8692.
42. Clingen, P. H., C. F. Arlett, L. Roza, T. Mori, O. Nikaido and M. H. L. Green (1995) Induction of cyclobutane pyrimidine dimers, pyrimidine(6-4)pyrimidone photoproducts, and Dewar valence isomers by natural sunlight in normal human mononuclear cells. *Cancer Res.* **55**, 2245–2248.
43. Banyasz, A., I. Vayá, P. Changenet-Barret, T. Gustavsson, T. Douki and D. Markovitsi (2011) Base pairing enhances fluorescence and favors cyclobutane dimer formation induced upon absorption of UVA radiation by DNA. *J. Am. Chem. Soc.* **133**, 5163–5165.
44. Markovitsi, D. (2016) UV-induced DNA damage: the role of electronic excited states. *Photochem. Photobiol.* **92**, 45–51.
45. Perdiz, D., P. Gróf, M. Mezzina, O. Nikaido, E. Moustacchi and E. Sage (2000) Distribution and repair of bipyrimidine photoproducts in solar UV-irradiated mammalian cells: possible role of Dewar photoproducts in solar mutagenesis. *J. Biol. Chem.* **275**, 26732–26742.
46. Douki, T., A. Reynaud-Angelin, J. Cadet and E. Sage (2003) Bipyrimidine photoproducts rather than oxidative lesions are the main type of DNA damage involved in the genotoxic effect of solar UVA radiation. *Biochemistry* **42**, 9221–9226.
47. Mouret, S., C. Baudouin, M. Charveron, A. Favier, J. Cadet and T. Douki (2006) Cyclobutane pyrimidine dimers are predominant DNA lesions in whole human skin exposed to UVA radiation. *Proc. Natl Acad. Sci. USA* **103**, 13765–13770.

48. Mouret, S., C. Philippe, J. Gracia-Chantegrel, A. Banyasz, S. Karpati, D. Markovitsi and T. Douki (2010) UVA-induced cyclobutane pyrimidine dimers in DNA: a direct photochemical mechanism? *Org. Biomol. Chem.* **8**, 1706–1711.

49. Wood, R. D. (1985) Pyrimidine dimers are not the principal pre-mutagenic lesions induced in lambda phage DNA by ultraviolet light. *J. Mol. Biol.* **184**, 577–585.

50. Otoshi, E., T. Yagi, T. Mori, T. Matsunaga, O. Nikaido, S. Kim, K. Hitomi, M. Ikenaga and T. Todo (2000) Respective roles of cyclobutane pyrimidine dimers, (6-4)photoproducts, and minor photoproducts in ultraviolet mutagenesis of repair-deficient xeroderma pigmentosum A cells. *Cancer Res.* **60**, 1729–1735.

51. Tanaka, M., S. Nakajima, M. Ihara, T. Matsunaga, O. Nikaido, and K. Yamamoto (2001) Effects of photoreactivation of cyclobutane pyrimidine dimers and pyrimidine (6-4) pyrimidone photoproducts on ultraviolet mutagenesis in SOS-induced repair-deficient *Escherichia coli*. *Mutagenesis* **16**, 1–6.

52. Mitchell, D. L., C. A. Haipek and J. M. Clarkson (1985) (6–4)Photoproducts are removed from the DNA of UV-irradiated mammalian cells more efficiently than cyclobutane pyrimidine dimers. *Mutat. Res.* **143**, 109–112.

53. Mitchell, D. L., J. E. Cleaver and J. H. Epstein (1990) Repair of pyrimidine(6-4)pyrimidone photoproducts in mouse skin. *J. Invest. Dermatol.* **95**, 55–59.

54. Ley, R. D., B. A. Sedita, D. D. Grube and J. M. Fry (1977) Induction and persistence of pyrimidine dimers in the epidermal DNA of two strains of hairless mice. *Cancer Res.* **37**, 3243–3248.

55. Vijg, J., E. Mullaart, G. P. van der Schans, P. H. M. Lohman and D. L. Knook (1984) Kinetics of ultraviolet induced DNA excision repair in rat and human fibroblasts. *Mutat. Res.* **132**, 129–138.

640 56. Ikehata, H. (2018) Mechanistic considerations on the wavelength-dependent variations
641 of UVR genotoxicity and mutagenesis in skin: the discrimination of UVA-signature from
642 UV-signature mutation. *Photochem. Photobiol. Sci.* **17**, 1861–1871.
643 57. Cannistraro, V. J. and J.-S. Taylor (2009) Acceleration of 5-methylcytosine deamination
644 in cyclobutane dimers by G and its implications for UV-induced C-to-T mutation
645 hotspots. *J. Mol. Biol.* **392**, 1145–1157.
646 58. Cannistraro, V. J., S. Pondugula, Q. Song and J.-S. Taylor (2015) Rapid deamination of
647 cyclobutane pyrimidine dimer photoproducts at TCG sites in a translationally and
648 rotationally positioned nucleosome *in vivo*. *J. Biol. Chem.* **44**, 26597–26609.
649 59. Grünwald, S. and G. P. Pfeifer (1989) Enzymatic DNA methylation. *Prog. Clin.*
650 *Biochem. Med.* **9**, 61–103.
651 60. Drouin, R. and J.-P. Therrien (1997) UVB-induced cyclobutane pyrimidine dimer
652 frequency correlates with skin cancer mutational hotspots in *p53*. *Photochem. Photobiol.*
653 **66**, 719–726.
654 61. Tommasi, S., M. F. Denissenko and G. P. Pfeifer (1997) Sunlight induces pyrimidine
655 dimers preferentially at 5-methylcytosine bases. *Cancer Res.* **57**, 4727–4730.
656 62. Ikehata, H. and T. Ono (2007) Significance of CpG methylation for solar UV-induced
657 mutagenesis and carcinogenesis in skin. *Photochem. Photobiol.* **83**, 196–204.
658 63. Rochette, P. J., S. Lacoste, J.-P. Therrien, N. Bastien, D. E. Brash and R. Drouin (2009)
659 Influence of cytosine methylation on ultraviolet-induced cyclobutane pyrimidine dimer
660 formation in genomic DNA. *Mutat. Res.* **665**, 7–13.
661 64. Qin, X., S. Zhang, H. Oda, Y. Nakatsuru, S. Shimizu, Y. Yamazaki, O. Nikaido and T.
662 Ishikawa (1995) Quantitative detection of ultraviolet light-induced photoproducts in
663 mouse skin by immunohistochemistry. *Jpn. J. Cancer Res.* **86**, 1041–1048.

65. Mouret, S., M. Charveron, A. Favier, J. Cadet and T. Douki (2008) Differential repair of UVB-induced cyclobutane pyrimidine dimers in cultured human skin cells and whole human skin. *DNA Repair* **7**, 704–712.
66. Pines, A., C. Backendorf, S. Alekseev, J. G. Jansen, F. R. de Gruijl, H. Vrieling and L. H. F. Mullenders (2009) Differential activity of UV-DDB in mouse keratinocytes and fibroblasts: impact on DNA repair and UV-induced skin cancer. *DNA Repair* **8**, 153–161.
67. Lu, Y., Y. Lou, P. Yen, D. Mitchell, M. Huang and A. H. Conney (1999) Time course for early adaptive responses to ultraviolet B light in the epidermis of SKH-1 mice. *Cancer Res.* **59**, 4591–4602.
68. Marsh, E., D. G. Gonzalez, E. A. Lathrop, J. Boucher and V. Greco (2018) Positional stability and membrane occupancy define skin fibroblast homeostasis *in vivo*. *Cell* **175**, 1620–1633.

676 **Figure legends**

677

678 **Figure 1.** Dose-response kinetics of DNA photolesion formation by monochromatic UVR. (a,
679 b) Dose-dependent formation kinetics of CPDs (a) and 64PPs (b) in the epidermis (open
680 circles) and dermis (open diamonds) in mouse skin after irradiation. Each data point was
681 derived from a single mouse. The colored points (red and blue for the epidermis and dermis,
682 respectively) were used for regression analysis (dotted lines) to evaluate the slopes of the
683 photolesion formation kinetics (shown equations). (c) Dose-dependent formation kinetics of
684 CPDs (open circles) and 64PPs (open diamonds) in naked DNA after irradiation. Each data
685 point was derived from a single DNA sample. The colored points (red and blue for CPDs and
686 64PPs, respectively) were used for regression analysis (dotted lines) to evaluate the slopes of
687 the photolesion formation kinetics (shown equations). The amounts of the photolesions were
688 evaluated through a quantitative ELISA using specific monoclonal antibodies for each
689 photolesion and standard UVR-damaged calibration DNA.

690

691 **Figure 2.** Wavelength dependence of UVR photolesion formation. (a) Action spectra of the
692 formation of CPDs (circle) and 64PPs (triangle) in DNA (black) and the mouse epidermis
693 (red) and dermis (blue). The error bars show the standard errors. (b) Comparisons of the action
694 spectra of the formation of each photolesion shown in (a) among naked DNA and skin tissues
695 in a single graph. (c) Wavelength dependence of molecular ratios of 64PPs to CPDs formed in
696 DNA and skin tissues.

697

698 **Figure 3.** Comparison of the action spectra between photolesion formation and mutagenesis in
699 the mouse skin. The action spectra of CPD (red) and 64PP (blue) formation in each mouse
700 tissue, epidermis and dermis, are overlaid in a single graph along with the action spectra of

mutagenicity (black) normalized at 300 nm. The mutagenicity data were derived from Ikehata *et al.* (20).

Figure 4. Molecular mutagenicity of CPD in mouse skin. (a) Wavelength dependence of the mutagenicity of a CPD molecule (CPD mutagenicity) in the mouse epidermis (red) and dermis (blue). (b) Wavelength dependence of the ratio of CPD mutagenicity in the epidermis to that in the dermis. This dependence was calculated from the data in (a).

Figure 5. Estimation of the ability of UVR photolesions to induce the MIS response. The minimum amounts of CPDs (red) and 64PPs (blue) necessary to induce the MIS response were determined at the wavelengths used for the analysis by deducing from the minimum MIS doses in the epidermis reported previously (20).

Fig. 1a

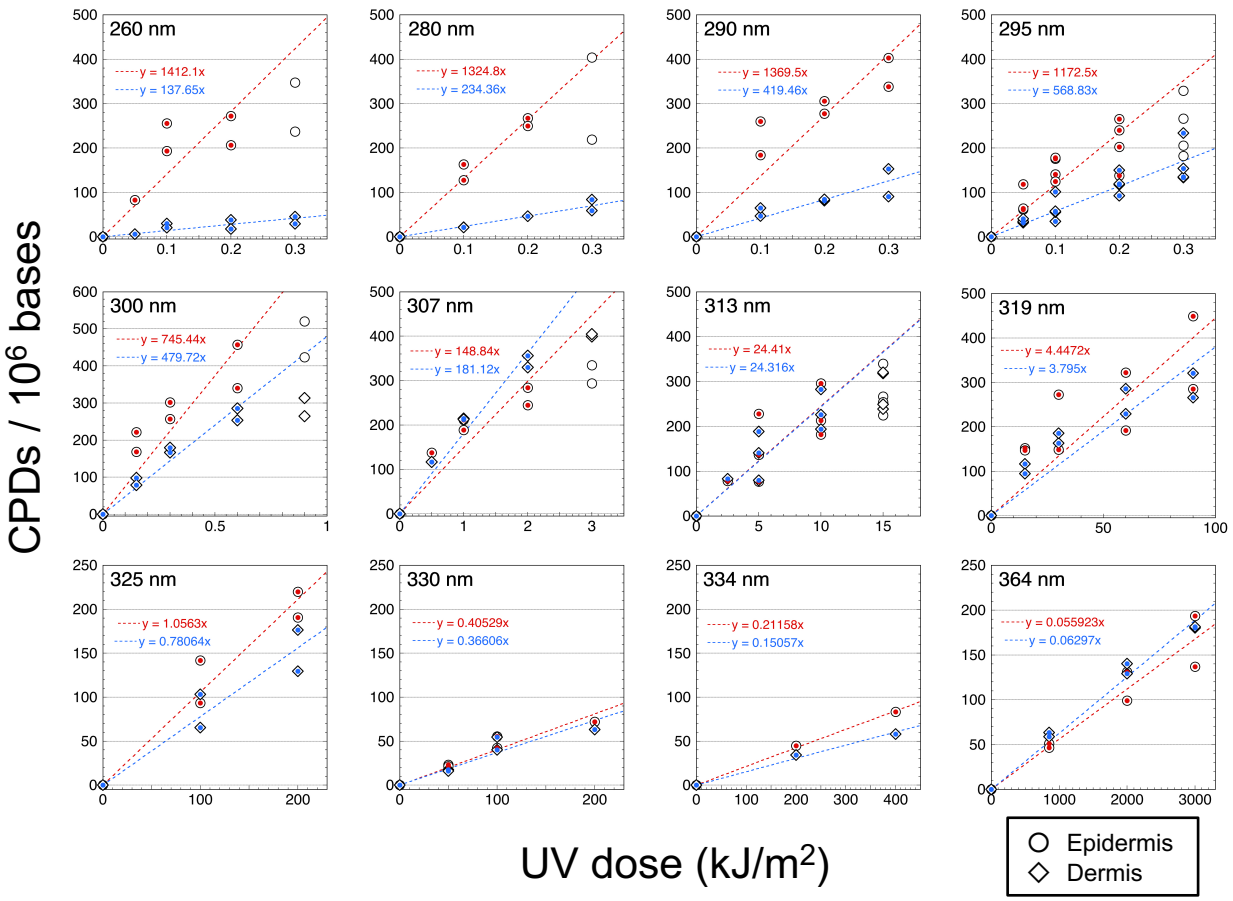
CPDs / 10^6 bases
UV dose (kJ/m^2)
260 nm
y = 1412.1x
y = 137.65x
280 nm
y = 1324.8x
y = 234.36x
290 nm
y = 1369.5x
y = 419.46x
295 nm
y = 1172.5x
y = 568.83x
300 nm
y = 745.44x
y = 479.72x
307 nm
y = 148.84x
y = 181.12x
313 nm
y = 24.41x
y = 24.316x
319 nm
y = 4.4472x
y = 3.795x
325 nm
y = 1.0563x
y = 0.78064x
330 nm
y = 0.40529x
y = 0.36606x
334 nm
y = 0.21158x
y = 0.15057x
364 nm
y = 0.055923x
y = 0.06297x
Epidermis
Dermis

Fig. 1b

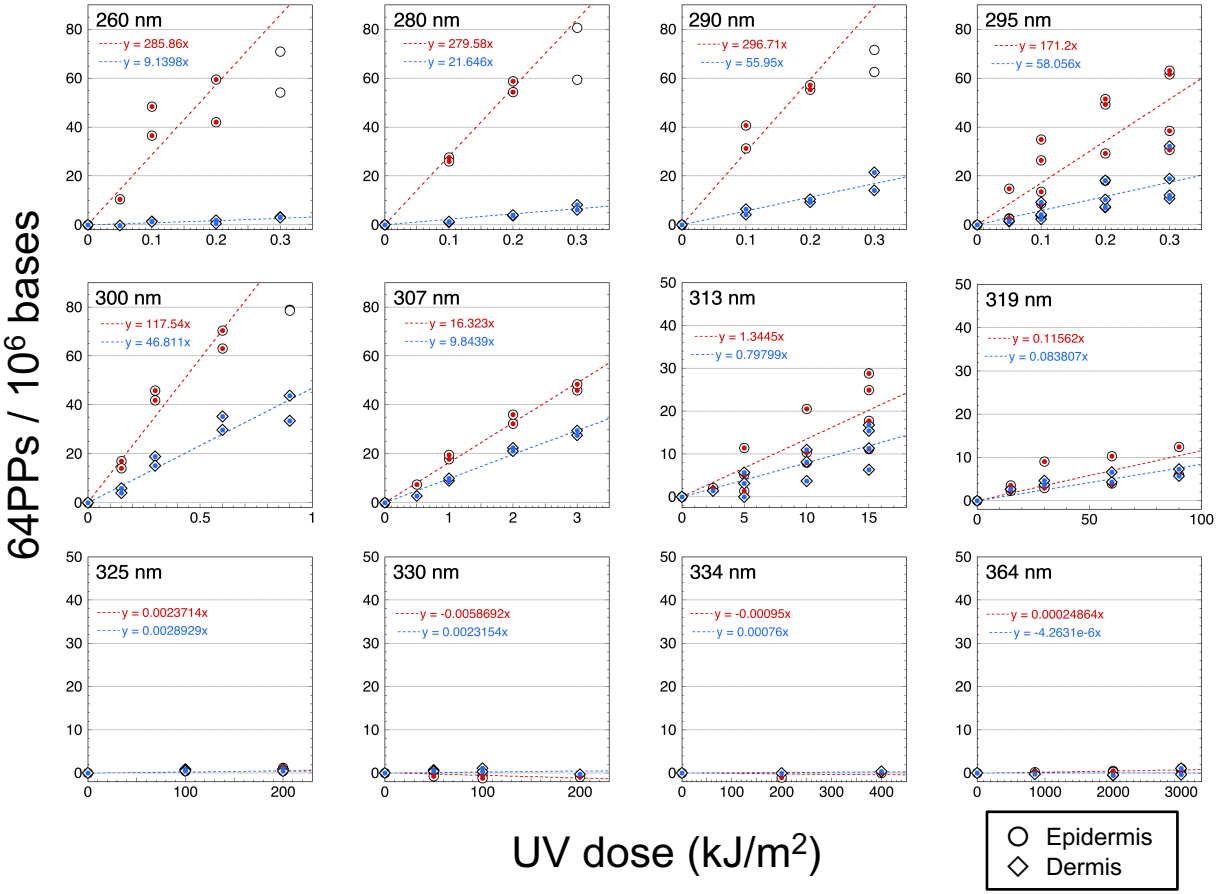
64PPs / 10^6 bases
260 nm
y = 285.86x
y = 9.1398x
280 nm
y = 279.58x
y = 21.646x
290 nm
y = 296.71x
y = 55.95x
295 nm
y = 171.2x
y = 58.056x
300 nm
y = 117.54x
y = 46.811x
307 nm
y = 16.323x
y = 9.8439x
313 nm
y = 1.3445x
y = 0.79799x
319 nm
y = 0.11562x
y = 0.083807x
325 nm
y = 0.0023714x
y = 0.0028929x
330 nm
y = -0.0058692x
y = 0.0023154x
334 nm
y = -0.00095x
y = 0.00076x
364 nm
y = 0.00024864x
y = -4.2631e-6x
UV dose (kJ/m2)
Epidermis
Dermis

Fig. 1c

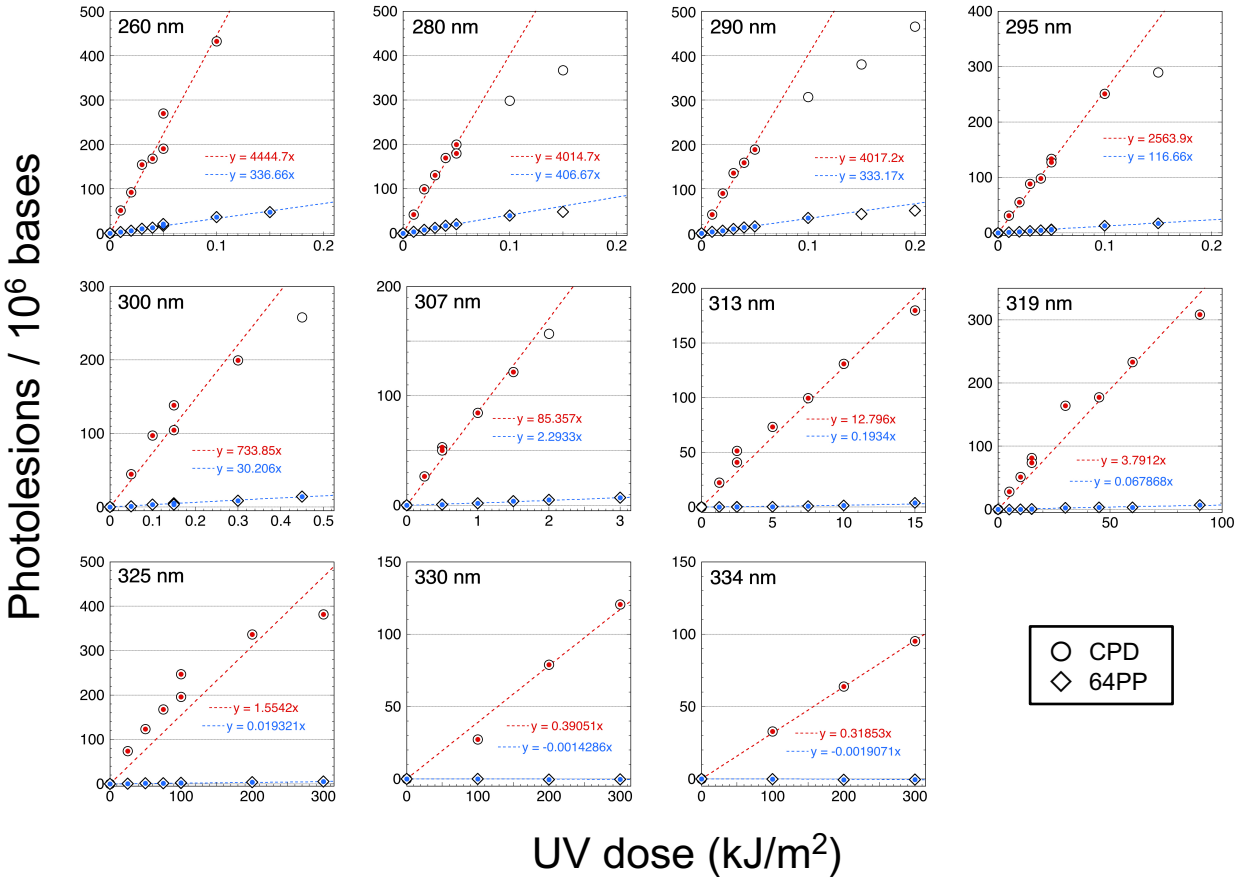
Photolesions / 10^6 bases
260 nm
y = 4444.7x
y = 336.66x
280 nm
y = 4014.7x
y = 406.67x
290 nm
y = 4017.2x
y = 333.17x
295 nm
y = 2563.9x
y = 116.66x
300 nm
y = 733.85x
y = 30.206x
307 nm
y = 85.357x
y = 2.2933x
313 nm
y = 12.796x
y = 0.1934x
319 nm
y = 3.7912x
y = 0.067868x
325 nm
y = 1.5542x
y = 0.019321x
330 nm
y = 0.39051x
y = -0.0014286x
334 nm
y = 0.31853x
y = -0.0019071x
CPD
64PP
UV dose (kJ/m2)

Fig. 2a

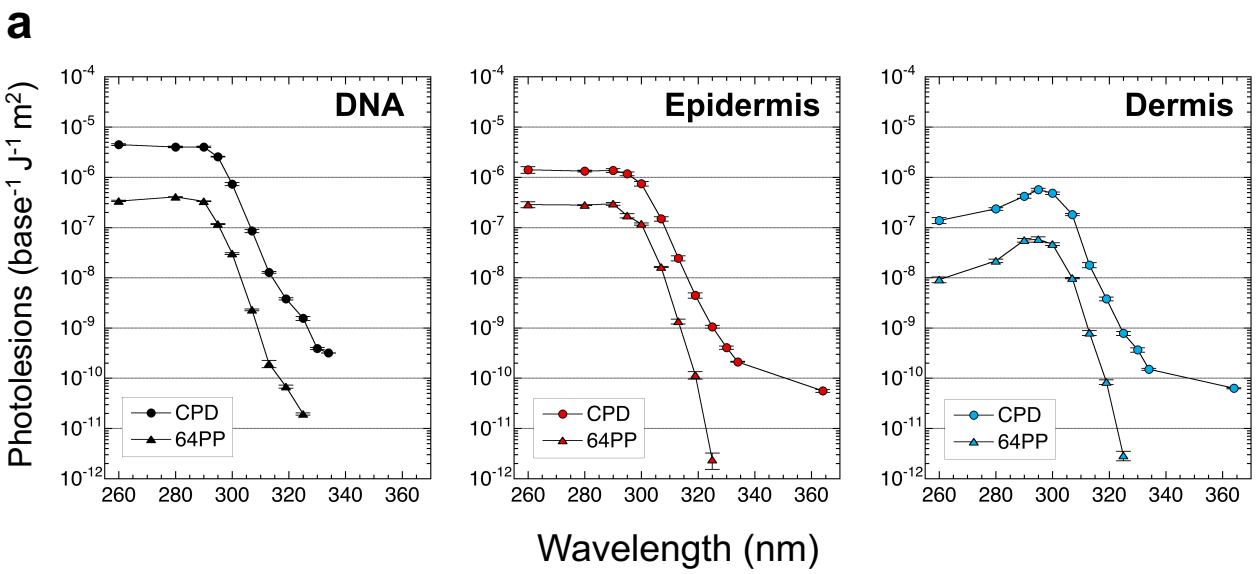
a
DNA
Epidermis
Dermis
CPD
64PP
Photolesions (base^{-1} J^{-1} m^2)
Wavelength (nm)
10^{-4}
10^{-5}
10^{-6}
10^{-7}
10^{-8}
10^{-9}
10^{-10}
10^{-11}
10^{-12}
260
280
300
320
340
360

Fig. 2b

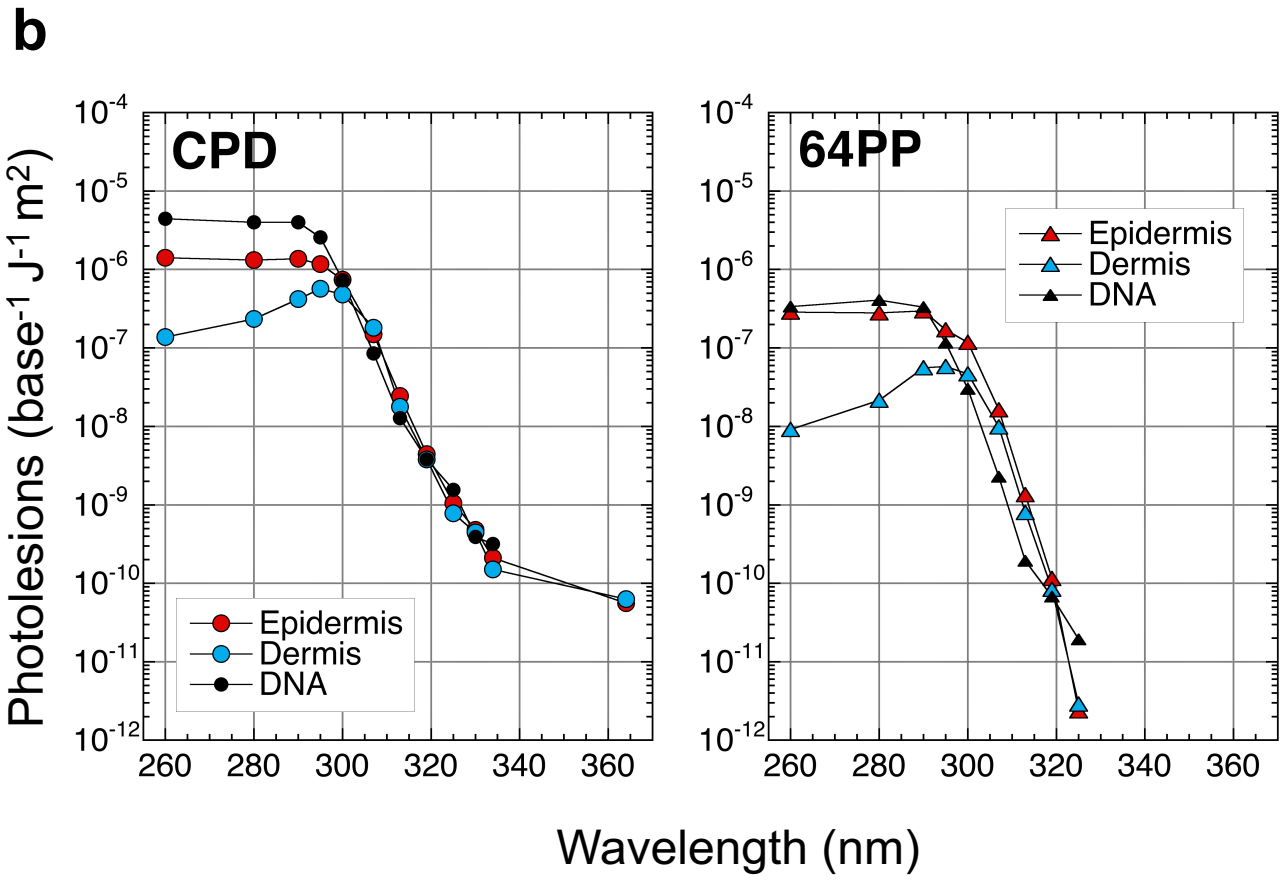
b
CPD
64PP
Epidermis
Dermis
DNA
Photolesions (base-1 J-1 m2)
Wavelength (nm)
10-4
10-5
10-6
10-7
10-8
10-9
10-10
10-11
10-12
260
280
300
320
340
360

Fig. 2c

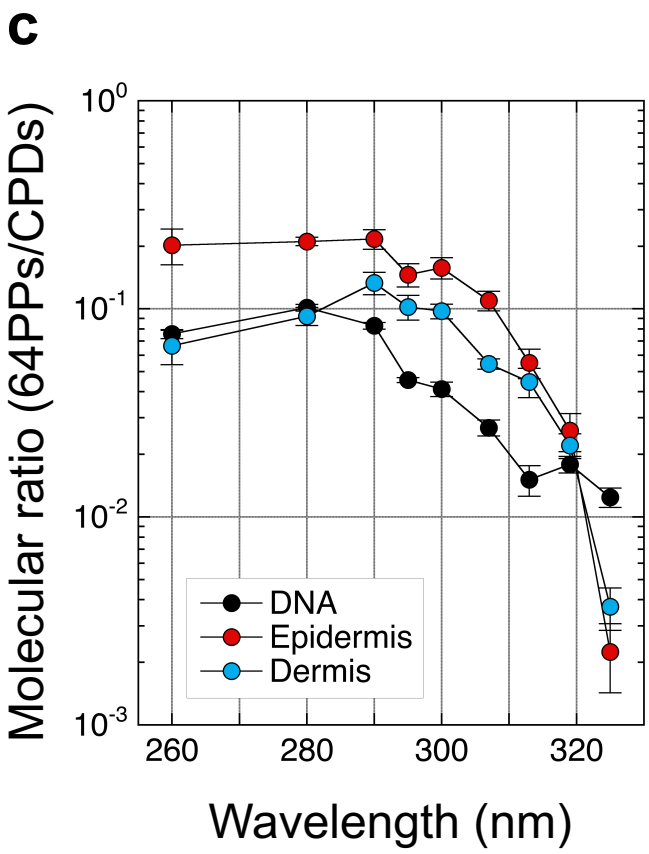
c
Molecular ratio (64PPs/CPDs)
10^0
10^{-1}
10^{-2}
10^{-3}
260
280
300
320
Wavelength (nm)
DNA
Epidermis
Dermis

Fig. 3

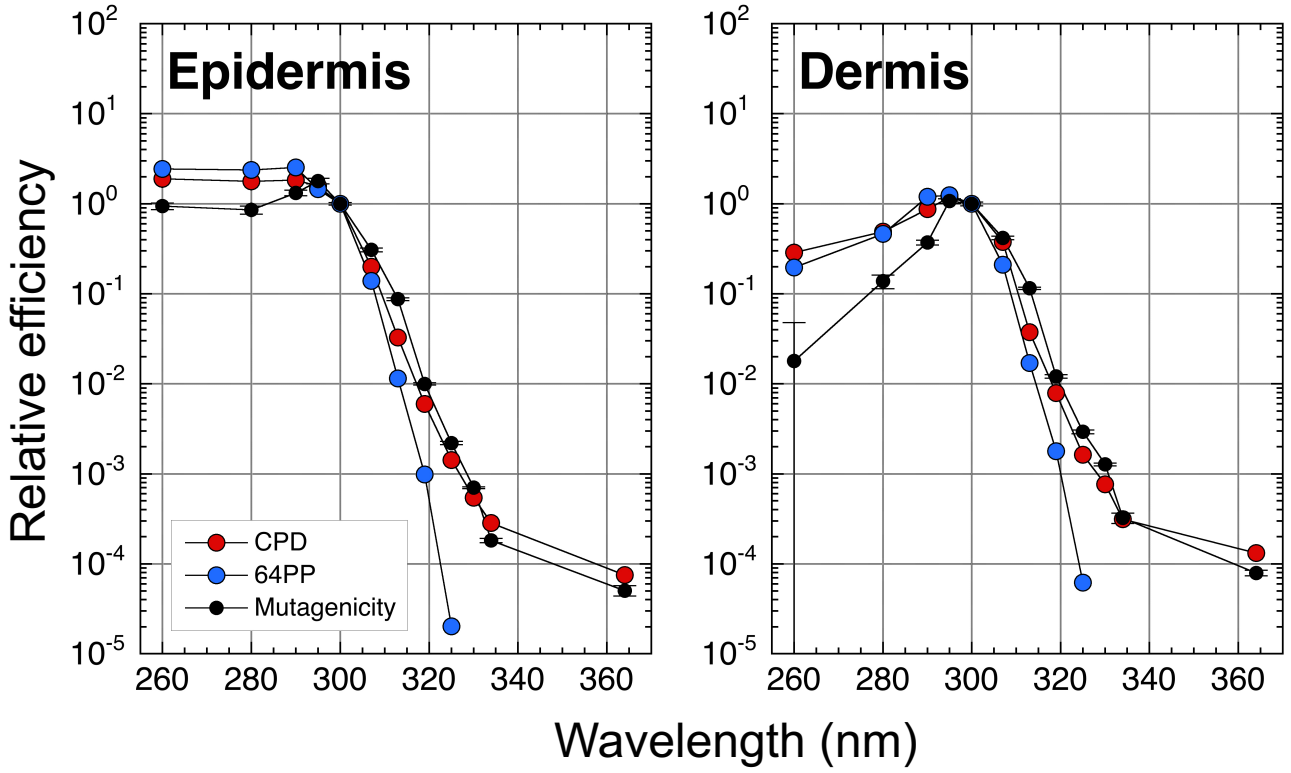
Epidermis
Dermis
Relative efficiency
Wavelength (nm)
CPD
64PP
Mutagenicity
10^{2}
10^{1}
10^{0}
10^{-1}
10^{-2}
10^{-3}
10^{-4}
10^{-5}
260
280
300
320
340
360

Fig. 4

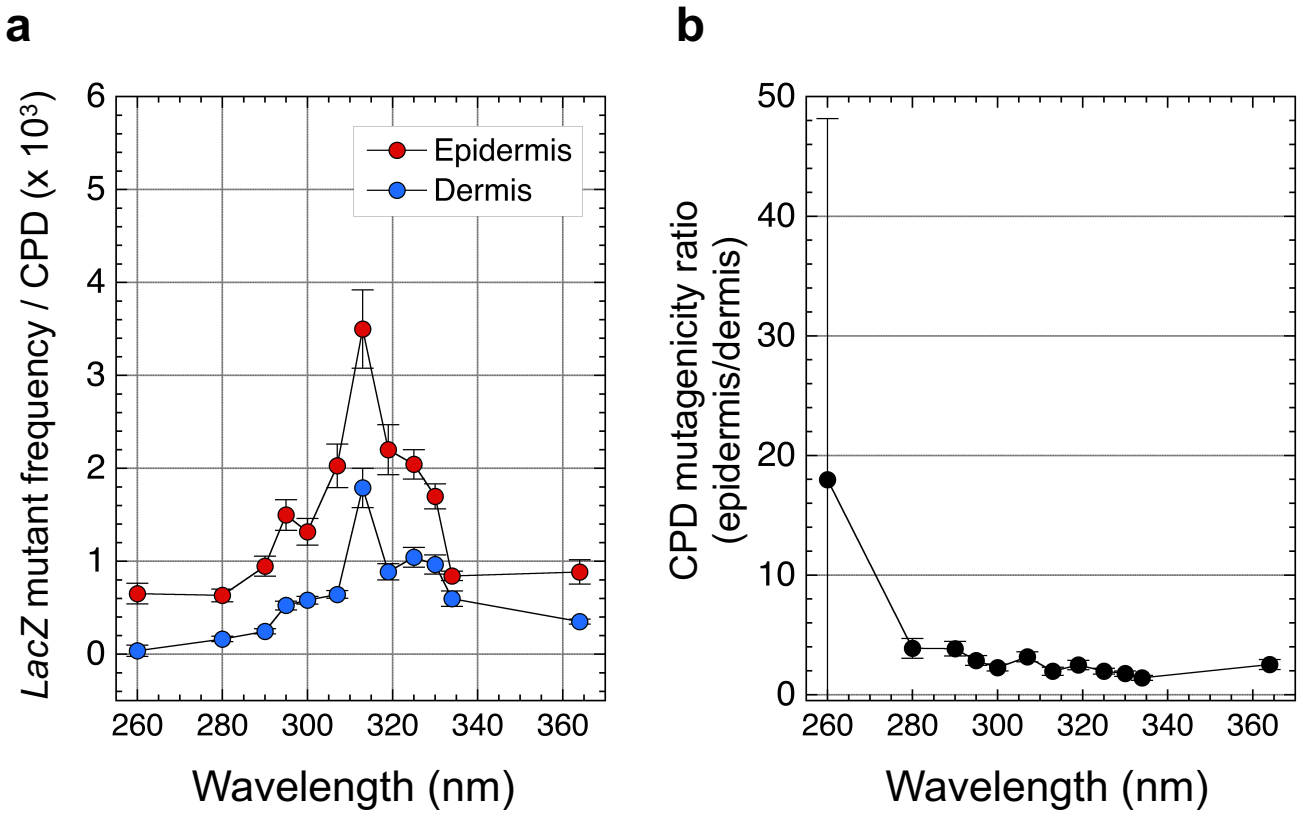
a
b
LacZ mutant frequency / CPD (x 10³)
Epidermis
Dermis
Wavelength (nm)
CPD mutagenicity ratio
(epidermis/dermis)
Wavelength (nm)

Fig. 5

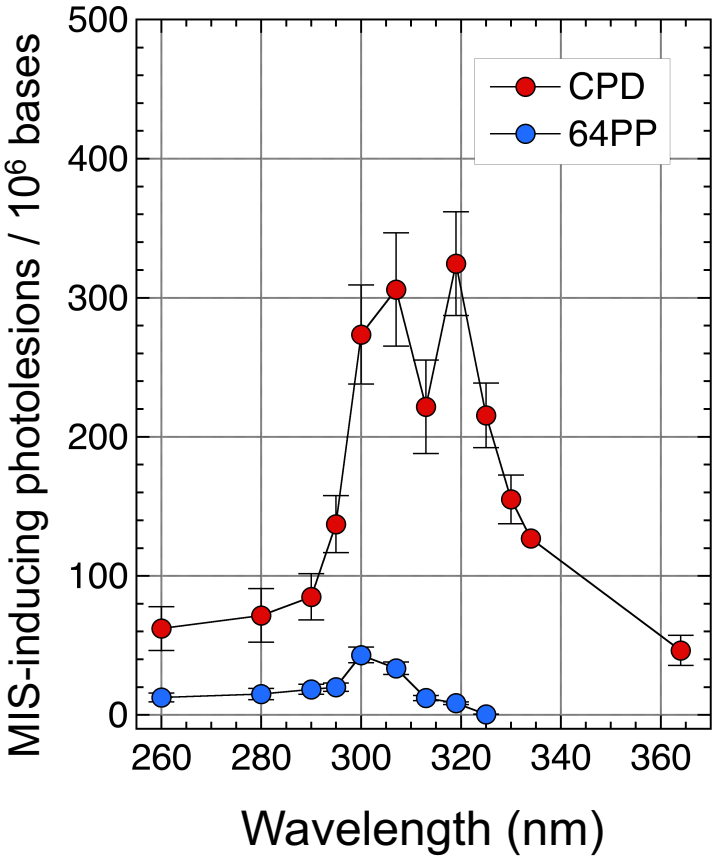
MIS-inducing photolesions / 10^6 bases
500
400
300
200
100
0
260
280
300
320
340
360
Wavelength (nm)
CPD
64PP